JOURNAL OF GEOPHYSICAL RESEARCH, VOL. 86, NO. B3, PAGES 1785–1793, MARCH 10, 1981

Effects of Fault Interaction on Moment, Stress Drop, and Strain Energy Release

J. W. RUDNICKI

Department of Theoretical and Applied Mechanics, University of Illinois, Urbana, Illinois 61801

H. KANAMORI

Seismological Laboratory, California Institute of Technology, Pasadena, California 91125

Solutions for collinear shear cracks are used to examine quantitatively the effects of fault slip zone interaction on determinations of moment, stress drop, and static energy release. Two models, the barrier model and the asperity model, are considered. In the asperity model, the actual distribution of strengths on a fault plane is idealized as a combination of two limiting cases: areas which slip freely at a uniform value of a residual friction stress and unbroken ligaments or 'asperities' across which slip occurs only at the time of a seismic event. In the barrier model, slip zones separated by unbroken ligaments (barriers) are introduced into a uniformly stressed medium to approximate the nonuniform fault propagation proposed by Das and Aki. The strain energy change due to introducing collinear slip zones or due to breaking the asperities between them is shown to be given by the usual formula for an isolated slip zone with the stress drop replaced by the effective stress. Significant interaction between slip zones occurs only if the length of the asperity is less than half the length of the slip zones. For the case of two collinear slip zones, fracture of the asperity between them is shown to cause a large moment primarily because of the additional displacement which is induced on the adjacent slip zones. For example, if the asperity length is $0.05l$, where l is the length of each adjacent slip zone, then fracture of the asperity causes a moment almost 1.8 times the moment caused by introducing a slip zone of length l. For two collinear slip zones, the local stress drop due to fracture of the separating asperity is shown to become unbounded as the asperity length goes to zero, but in the same limit the stress drop averaged over the entire fault length is approximately equal to the apparent stress drop inferred for an isolated fault of the same moment and total fault length. This apparent stress drop is approximately equal (within a factor of 2 or 3) to the effective stress and hence can be used in the usual formula to give a good estimate of the strain energy change. For the barrier model, numerical results are given for the ratio of the stress drop calculated on the assumption of an isolated slip zone to the true stress drop. For example, in the case of two collinear slip zones of length l separated by a barrier of length $0.2l$, this ratio is 0.5, whereas for a barrier length equal to that of the adjacent slip zones, the ratio is 0.24. Stress drop estimates become worse with increasing number of fault segments.

INTRODUCTION

Although earthquake faulting is often idealized as smoothly varying slip on an isolated zone, it has become increasingly evident from detailed analysis of seismograms that slip on earthquake faults is very irregular. This irregularity is particularly evident in large earthquakes which have been shown to consist of a number of distinct events [e.g., *Imamura,* 1937; *Miyamura et al.,* 1964; *Wyss and Brune,* 1967; *Trifunac and Brune,* 1970; *Nagamune,* 1971]. More recent studies on the waveforms of these multiple shocks have unravelled some of the details of the stress release in these complex events [e.g., *Kanamori and Stewart,* 1978; *Rial,* 1978]. Also, the occurrence and distribution of foreshocks [*Jones and Molnar,* 1979; *Ishida and Kanamori,* 1978, 1980] and doublet earthquakes [*Lay and Kanamori,* 1980] have been used to infer patterns of fault plane heterogeneity. Thus it seems likely that the distribution of slip and stress on fault planes is very heterogeneous. For faults that have previously undergone large amounts of slip, the stress on much of the fault plane may be equal to a residual value of the friction stress. However, there are also likely to be regions having higher resistance to slip. These regions are usually termed 'asperities' (this term is not meant to be interpreted in the specific sense in which it is used in the physics of friction of referring to a geometric surface roughness [e.g., *Bowden and Tabor,* 1973]), and they may be due to either material or geometric effects.

In the interpretation of these multiple shocks, it is often assumed, implicitly or explicitly, that the individual events in the multiple-shock sequence represent failure of such asperities. In the following discussion we refer to this type of faulting as the asperity model. Furthermore, it has been suggested [*Kanamori,* 1978; *Das and Aki,* 1977*b*; *Aki,* 1979; *Mikumo and Miyatake,* 1979; *Ishida and Kanamori,* 1978, 1980; *Lay and Kanamori,* 1980] that asperities may control the pattern of earthquake occurrence, for example, foreshock-mainshock, swarm, doublet, etc.: as tectonic stress is increased, weaker asperities fail and the resulting slip alters the stress in the remaining stronger asperities.

On the other hand, *Das and Aki* [1977*b*] have suggested, on the basis of numerical experiments in dynamic crack propagation, that a propagating fault may leave behind unbroken barriers, that is, high-strength areas of the fault plane. They called this type of faulting the barrier model. Several authors [*Madariaga,* 1979; *Rice,* 1979*b*; *Aki,* 1979] have shown that seismic parameters inferred by assuming uniform slip or stress drop can be in considerable error if the earthquake is represented by the barrier model.

Although these two models would represent the two extreme cases of the actual earthquake process, they are useful for characterizing fault plane heterogeneity.

Madariaga [1979] has given an elegant formula relating

Copyright © 1981 by the American Geophysical Union.

Paper number 80B1382.
0148-0227/81/080B-1382$01.00

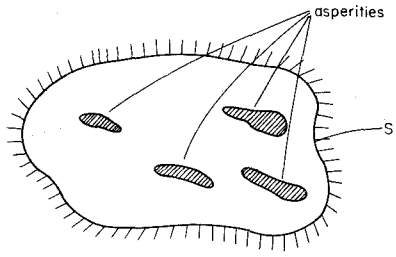

Fig. 1. Schematic idealization of a fault plane. Outside the curve labeled S there is no relative displacement of the fault surfaces. Inside curve S the fault surfaces slip freely at a residual friction stress except for the cross-hatched areas which represent 'asperities' across which there is relative displacement only during seismic events.

stress drop and moment under general circumstances, and he uses this to give some approximate results for a few special cases. It is, however, a matter of practical interest to determine the magnitude of effects of fault zone interaction on moment, static stress drop, and strain energy change. This paper examines quantitatively these effects primarily by using the asperity model.

We idealize the distribution of strengths on the fault plane as a combination of the following two limiting cases: locked segments which slip only at the time of a seismic event and segments which freely slip at a residual friction stress. As a more specific illustration, consider the idealized fault plane shown in Figure 1. The region outside the curve labeled S is idealized as locked. Inside curve S, the cross-hatched areas are also locked and represent asperities or portions of the fault which require a greater level of applied stress in order for slip to occur. The remainder of the fault inside curve S sustains a uniform friction stress τ_f but slips freely at stresses larger than τ_f. This model can be further idealized as a distribution of plane (or antiplane) strain (i.e., of infinite extent in one direction) shear cracks as shown in Figure 2. The variations along the fault plane of stress and of relative slip are shown schematically. The cracks model slip zones which sustain the uniform friction stress τ_f, and the ligaments between the cracks (slip zones) represent asperities.

Although this model is oversimplified, it has the advantage that existing results for collinear cracks can be used to obtain exact, closed-form expressions which make possible a quantitative assessment of the effects due to the interaction of slip zones. Because the idealization is a limiting one, the results given here can reasonably be expected to yield bounds for more realistic situations. Moreover, the results provide some specific numerical examples of the general relations between moment and stress drop derived by *Madariaga* [1979] and illustrate the extent to which small strong asperities or barriers can control the pattern of stress release. Although many of the general results illustrated here are well known, for example, that stress drop in a small asperity will exceed the average stress drop, the numerical results permit a quantitative assessment of the magnitude of these effects and the extent to which they depend on the separation distances of slip zones and asperities or barriers.

The next section discusses some preliminary considerations and reviews some results for isolated slip zones before considering the interaction of slip zones separated by asperities.

Some Results for Isolated Slip Zones

Consider an isolated slip zone of length l which is embedded in an infinite linear elastic body (Figure 3). For convenience, the slip zone is considered to be of infinite extent in one direction so that plane strain conditions apply. The slip zone sustains a uniform frictional stress τ_f and the body is loaded in the far field by the shear stress τ_∞. The stresses near the ends of such a slip zone are proportional to $r^{-1/2}$, where r is the distance from the edge of the zone, and are characterized by the stress intensity factor K [e.g., *Knott*, 1973; *Rice*, 1968], which is defined by the following relation:

$$K = \lim_{r \to 0} (2\pi r)^{1/2} \sigma_{xy} \tag{1}$$

where σ_{xy} is the shear stress on the plane ahead of the slip zone. If the slip zone shown in Figure 3 encloses no net dislocation (so that the displacement field outside the zone is single valued), the stress intensity factor is

$$K_i = (\pi l/2)^{1/2}(\tau_\infty - \tau_f) \tag{2}$$

where the subscript denotes the value for an isolated slip zone.

Of course, in any real material, the stresses at the edge of the slip zone will not be singular but instead will be alleviated by processes of inelastic deformation. If, however, the characteristic dimension of this zone of inelasticity or 'breakdown' zone is small by comparison with other length scales in the problem (e.g., length of slip zone, distance to boundaries, etc.), then the intensity of deformation in this zone is characterized by K. More precisely, the boundary conditions on the breakdown zone are fixed by the singular stress of the surrounding linear elastic field. In the absence of any detailed information about processes in the breakdown zone, the near-tip stress field can be idealized as singular with the understanding that K characterizes the actual near-tip field (*Rice* [1968]; also see *Rudnicki* [1980] for a recent discussion).

Note that a uniform stress $-\tau_\infty$ or $-\tau_f$ may be superposed on the stress field in Figure 3 without affecting the relative displacement of the fault surfaces. Hence the relative displacement may be regarded as due to the application of stresses $\tau_\infty - \tau_f$ to the fault surfaces with zero stress at infinity or to application of stresses $\tau_\infty - \tau_f$ at infinity with a frictionless fault surface. In any case the relative displacement is

$$\delta_i(x) = 2(1 - \nu)\tau\mu^{-1}[(l/2)^2 - x^2]^{1/2} \tag{3}$$

where $\tau = \tau_\infty - \tau_f$ is the effective stress (which is equal in this case to the stress drop), μ is the shear modulus, ν is Poisson's ratio, and the subscript again denotes the value for an isolated slip zone. The average relative slip is

$$\bar{\delta}_i(l) = \pi(1 - \nu)\tau\mu^{-1}l/4 \tag{4}$$

The static moment (per unit thickness) is

$$M = \int_{-l/2}^{l/2} \mu\delta(x)\, dx \tag{5}$$

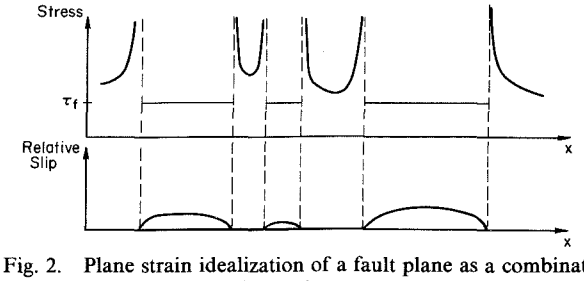

Fig. 2. Plane strain idealization of a fault plane as a combination of areas which freely slip at the friction stress τ_f and areas of asperities which undergo no relative displacement.

where the integration limits imply that the coordinate origin is at the crack center, or, for constant μ,

$$M = \mu l \bar{\delta} \tag{6}$$

Substituting from (4) yields

$$M_i(l) = (1 - \nu)\tau\pi(l/2)^2 \tag{7}$$

for the isolated slip zone. In this formula it is, of course, the seismic moment which is determined most accurately from observations. The stress drop τ is typically inferred from (7) or a similar formula on the basis of the observed moment and the observed or estimated fault length. As has been discussed in detail by *Madariaga* [1977], this stress drop is not generally equal to the average of the true stress drop. However, it will be shown that for the geometry considered here the difference between these quantities is not great.

Strain Energy Change

Although the strain energy change during faulting cannot, in general, be determined (because the friction on the fault is unknown), the strain energy change does provide an upper bound to the energy available for seismic wave radiation. The strain energy change caused by introducing the slip zone can be computed as the negative of the work done by the fault surface tractions in restoring the body to the unslipped state [*Rice*, 1966]. If the stress on the fault is reduced to the residual friction stress τ_f, this work is

$$W = \tau_f \bar{\delta} l + \frac{1}{2}\int_{-l/2}^{l/2} \Delta\tau(x)\, \delta(x)\, dx \tag{8}$$

where $\Delta\tau(x)$ is the stress drop. For the isolated zone, $\Delta\tau(x) = \tau_\infty - \tau_f$ and, consequently,

$$W = \tau_f l \bar{\delta} + \tfrac{1}{2}(\tau_\infty - \tau_f) l \bar{\delta} \tag{9}$$

The usual interpretation of this equation is that the first term is equal to the heat generated by faulting [e.g., *Orowan*, 1960] and the second term is available for seismic energy radiation. Comparison of (6) with (9) reveals that this second term, which *Kanamori* [1977] calls W_0, can be expressed in terms of the moment as

$$W_0 = \tau M/2\mu \tag{10}$$

where $\tau = \tau_\infty - \tau_f$. Of course, the actual seismic energy radiated during faulting depends on the deatils of the rupture process (whereas the strain energy change does not; this will be demonstrated below for the specific model considered here) and cannot be determined from comparison of the static

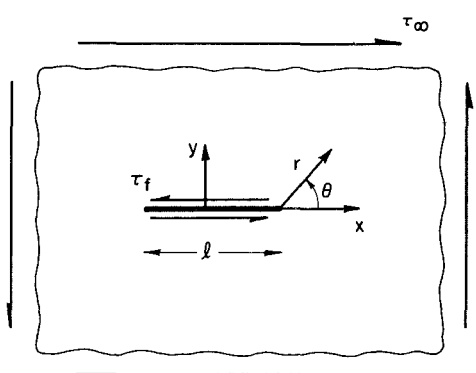

Fig. 3. An isolated slip zone. The resistive frictional stress is τ_f, and the slip zone is loaded in the far field by τ_∞.

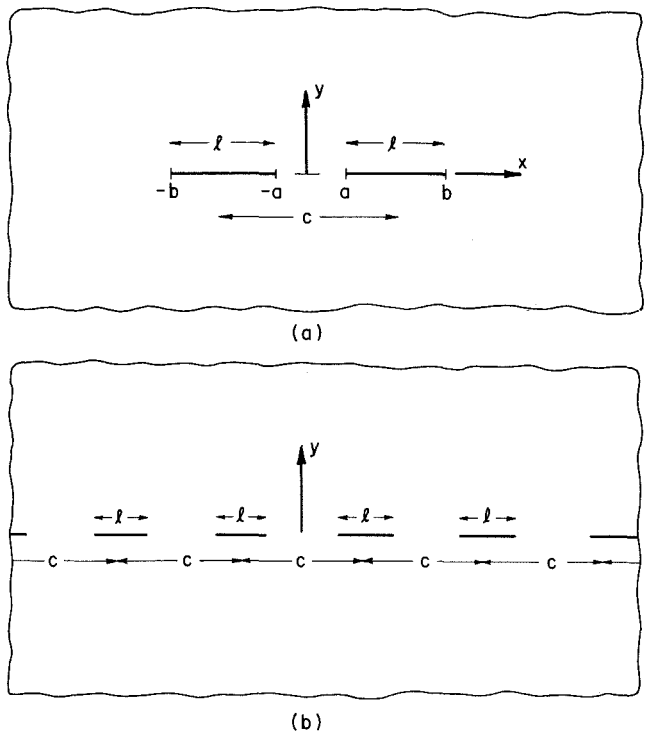

Fig. 4. (*a*) Geometry for two collinear slip zones. (*b*) Geometry for an infinite periodic array of collinear slip zones.

end-states [*Kostrov*, 1974]. However, *Kanamori* [1977] has shown that for large earthquakes the energy computed from (10) agrees well with the energy determined by using the observed magnitude and the Gutenberg-Richter relation (See *Richter* [1958] with correction noted by *Kanamori and Anderson* [1975].) In the following, we show that the strain energy change is also given by (9) for two specific types of nonuniform faulting.

First, we consider an initially unbroken fault. Then failure occurs on an array of collinear slip zones separated by ligaments as shown schematically in Figure 2. This case corresponds to the barrier model. The strain energy change is still given by (8) if the total length of the fault zone is l. Although the slip is very nonuniform, wherever the relative slip is nonzero the stress drop is equal to the effective stress $(\tau_\infty - \tau_f)$, and consequently (8) again reduces to (9).

In the second case we suppose that the fault plane is already segmented in the initial state and failure of the asperities causes reduction of the stress to τ_f everywhere on a zone of length l. This case corresponds to the asperity model. Again the pattern of stress drop is very complex: it is zero on portions of the fault plane which already sustained the residual friction stress τ_f, but it is nonzero and spatially varying where asperities existed. Nevertheless, the strain energy change is again given by (8). Note, however, that wherever the stress drop is nonzero (at positions which were occupied by asperities), the relative slip is exactly equal to the relative displacement for an isolated zone of length l. Hence $\delta(x)$ in the second term of (8) may, in this case, be replaced by $\delta_i(x)$ from (3). The reciprocal theorem of linear elasticity (e.g., *Love* [1927]; also see *Madariaga* [1979] for a more detailed treatment of a similar application of the reciprocal theorem) requires that

$$\int_{-l/2}^{l/2} (\Delta\tau)_i\, \delta(x)\, dx = \int_{-l/2}^{l/2} \Delta\tau(x)\, \delta_i(x)\, dx$$

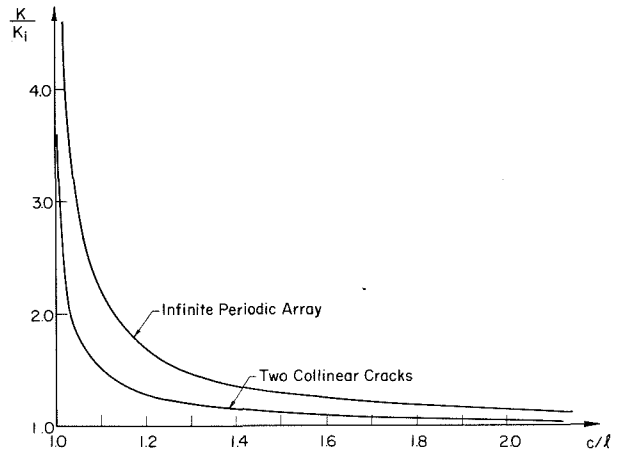

Fig. 5. Plot of stress intensity factor for fault tip at $x = \pm a$ in Figure 4*a* (equation (11)) and for Figure 4*b* (equation (12)) as a function of c/l.

where the subscript i in the first integral denotes the stress drop for an isolated slip zone. The stress drop for an isolated zone is, however, uniform and equal to the effective stress so that the strain energy change can again be expressed as in (9).

These examples demonstrate that for a fault zone of a given length, which may comprise any number of collinear slip zones, the strain energy change is fully determined by the effective stress and the average displacement regardless of the detailed distribution of constituent slip zones or of stress drop. Although this result is fully expected from the theory of linear elasticity, it often seems to be overlooked in seismology. The apparent reason for this is that the actual stress drop, which appears in the second term of (8), is not known but must be inferred from formulae like (7). Hence calculations based on (10) reflect possible inaccuracies in determining the stress drop by assuming an isolated slip zone with uniform stress drop.

Before proceeding to specific calculations of moment and stress drop for collinear slip zones, we present some results for the interaction of slip zone stress fields.

Interaction of Slip Zone Stress Fields

Although the solution for an arbitrary configuration of collinear cracks can formally be established using the powerful complex variable methods of *Muskhelvishvili* [1953], only the limiting cases of two collinear cracks [*Willmore,* 1949; *Tranter,* 1961; *Barenblatt,* 1962; *Erdogan,* 1962, *Lowengrub and Srivastava;,* 1968] and an infinite periodic array of collinear cracks [*Irwin,* 1957; *Koiter,* 1959] need be considered here. The solutions for these cases (and for many others) have been summarized by *Tada et al.* [1973]. For two collinear cracks, the geometry is shown in Figure 4*a*. The stress intensity factor at the interior fault tip ($x = \pm a$) is given by

$$K_2 = \tau(\pi a)^{1/2} \frac{b^2 E(m)/F(m) - a^2}{a(b^2 - a^2)^{1/2}} \tag{11}$$

where $\tau = \tau_\infty - \tau_f$ is the excess of the far field stress over the frictional stress, $m^2 = 1 - a^2/b^2$, and $F(m)$ and $E(m)$ are complete elliptic integrals of the first and second kinds, respectively:

$$F(m) = \int_0^{\pi/2} (1 - m^2 \sin^2\theta)^{-1/2}\, d\theta$$

$$E(m) = \int_0^{\pi/2} (1 - m^2 \sin^2\theta)^{1/2}\, d\theta$$

The center-to-center distance between the slip zones is $c = a + b$ and the length of each zone is $l = b - a$. The geometry for the infinite periodic array of slip zones is shown in Figure 4*b*, and the stress intensity factor is

$$K_\infty = \tau[c \tan(\pi l/2c)]^{1/2} \tag{12}$$

The interaction between the stress fields can be evaluated by examination of Figure 5, which plots K_2 and K_∞ divided by K_i, the stress intensity factor for an isolated crack, as a function of c/l. Figure 5 makes it clear that interaction is significant only when the slipping zones are very close together. This result is not unexpected, since the stress field near the tip of the slip zone does die off rapidly (as $r^{-1/2}$) with distance. The elevation of the stress intensity factor over the value of the isolated slip zone is, of course, greatest for the infinite array of slip zones. Even for this configuration, however, the stress intensity factor is greater than K_i by only slightly more than 10% when the zones are separated by a distance equal to their length ($c/l = 2$). Hence for greater separations, say, $c/l > 3$, the slip zones are effectively isolated. Although the interaction may be amplified by three-dimensional effects, the results here suggest that interaction is significant only if the asperities or locked portions occupy a small fraction of the fault plane.

A lower limit to the ratio of asperity length to slip zone length can be estimated by requiring that the average stress in the asperity which is available for release in a seismic event does not exceed the ultimate (peak) strength of brittle rock. (*Aki* [1979] has made similar estimates within the context of the barrier model.) For an asperity which has a length small by comparison to the lengths of adjacent slip zones, the stress in the asperity can be approximated by the singular term in the crack-tip expansion, that is, $K(2\pi r)^{-1/2}$, where K is the ap-

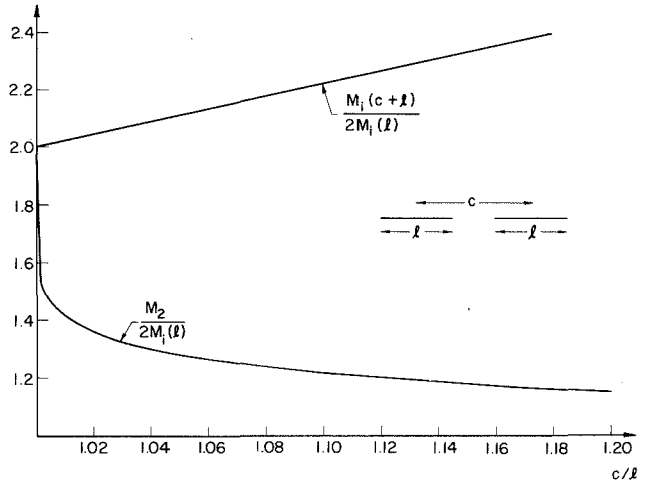

Fig. 6. Moment due to the introduction of two collinear slip zones of length l divided by 2 times the moment due to introduction of an isolated slip zone of length l plotted as a function of c/l (see (16) and (7)). Also shown is the moment for an isolated zone of length l divided by that for an isolated zone of length $c + l$.

propriate stress intensity factor and r is the distance from the edge of the slip zone. Thus the average stress in an asperity of length $c - l$ is

$$\bar{\sigma} = \tau(K/K_i)[c/l - 1]^{-1/2} \tag{13}$$

where the numerator and denominator have been multiplied by K_i, the stress intensity factor for an isolated slip zone, and $\tau = \tau_\infty - \tau_f$ is the effective stress. (Equation (13) actually gives an estimate of the stress in excess of the residual friction value.) Rearranging and setting $\sigma = \sigma_{ult}$, the ultimate stress, yield

$$\frac{c}{l} = 1 + \left(\frac{K}{K_i}\frac{\tau}{\sigma_{ult}}\right)^2 \tag{14}$$

although, of course K/K_i itself depends on c/l as shown in Figure 5. On the basis of laboratory experiments [e.g., *Jaeger and Cook*, 1976], a representative value for σ_{ult} might be 10^3 bars (=10^2 MPa), and τ is presumably in the range of typical stress drops, say, 10–100 bars (1–10 MPa). For τ/σ_{ult} equal to 10^{-2} and 10^{-1}, (14) yields values of c/l equal to 1.006 and 1.068, respectively, for the infinite periodic array. The corresponding values of c/l for two collinear cracks are 1.003 and 1.038. Hence $c/l = 1.006$ seems to be a reasonable lower limit.

Of course, the above estimates assume that the asperity remains essentially elastic and because of the proximity of the slip zones needed to cause significant interaction, it is worthwhile reexamining the adequacy of this assumption. As mentioned earlier, the formulation which regards the fault-tip stress field as singular is equivalent to one which takes explicit account of departures from linear elasticity in a breakdown zone as long as the characteristic length of this zone is small by comparison with other lengths in the problems. *Rice* [1979*a*] has estimated breakdown zone sizes from 11 mm to 1 m based on laboratory experiments of sliding friction. If these results are representative, it seems likely that the asperity size will be much greater than the end zone size. For a slip zone length of 1 km and the lower limit for $c/l = 1.006$, the asperity length is 6 m. *Rudnicki* [1979], however, has suggested, based on model experiments of *Barton* [1972, 1973], that larger end zone sizes, perhaps of the order of a hundred meters, may occur in situ, and it is conceivable that asperities may be of this size. Unfortunately, there seem to be no accurate estimates of sizes of either asperities or breakdown zones in the field, and *Rudnicki* [1980] has discussed the difficulties of extrapolating friction experiments to the field. In view of these uncertainties, the approximation of a singular stress field seems adequate. In any case, the stress field which is given by the resulting values for the stress intensity factors can be expected to describe adequately the average stress level in the asperity.

MOMENT AND STRESS DROP

Since the results are very different for the two models, the barrier and the asperity models, we discuss them separately. In the barrier model we compare the calculated moment and stress drop for the introduction of a segmented fault into a uniform state of stress with the corresponding quantities for an isolated fault or slip zone. In the asperity model the moment and stress drop due to failure of an asperity between existing slip zones are calculated. (Here 'failure' means that the stress is reduced to the residual friction value τ_f.) Again the results are compared with those for isolated slip zones. As

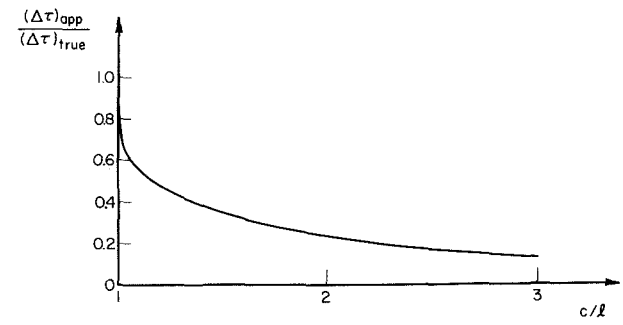

Fig. 7. Apparent stress drop (based on the assumption of an isolated slip zone) divided by actual stress drop for a fault having two segments of length l separated by the center-to-center distance c.

demonstrated earlier, the strain energy change and hence W_0 is completely determined, for a given fault length and effective stress, by the average displacement and consequently by the moment from (10). Thus despite the evident importance of W_0 as a seismological parameter, the results here have been expressed in terms of moment and stress drop because the moment can be determined more directly from observations and because errors in the estimation of W_0 (say, from (10)) result from errors in the stress drop.

Barrier Model

The moment due to introducing two widely separated slip zones of length l is simply $2M_i(l)$, where M_i is given by (7). As the two slip zones become closer together, the moment increases and the limiting value occurs when the slip zones are adjacent so that they approach a single zone of length $2l$. In this limit the moment is $M_i(2l) = 4M_i(l)$. For intermediate cases it is necessary to evaluate the moment by using (5). For the two collinear slip zones shown in Figure 4*a*, the relative slip of the fault surfaces can be determined from expressions given by *Erdogan* [1962] and, as shown in the appendix, the average slip is

$$\delta_2 = \pi(1 - \nu)\tau\mu^{-1}b\,\frac{[1 + (a/b)^2 - 2\lambda^2]}{2(1 - a/b)} \tag{15}$$

where $\lambda^2 = E(m)/F(m)$ and $m^2 = 1 - a^2/b^2$. Hence from (5) the moment is

$$M_2 = 2\pi(1 - \nu)\tau(b/2)^2[1 + (a/b)^2 - 2\lambda^2] \tag{16}$$

M_2 divided by twice the moment for an isolated zone of length $l = b - a$ is plotted in Figure 6 as a function of c/l (where $c = a + b$). As shown in Figure 6, $M_2 = 4M_i$ when $c/l = 1$ (i.e., $a/b = 0$) and M_2 approaches $2M_i$ as c/l approaches infinity (i.e., $a/b = 1$). Also plotted is $M_i\,(c + l)/2\,M_i(l)$. Figure 6 demonstrates that the effect of interaction is very slight unless the ratio of asperity size to slip zone length is extremely small. For example, for $c/l = 1.2$ (ratio of asperity length to slip zone length is 0.2), the moment M_2 differs by only 15% from the combined moments of two isolated zones of length l; for $c/l = 2.0$, the difference is only about 3%.

In calculating the moment it was assumed that the stress drop for each fault segment was $\tau_\infty - \tau_f$. However, as noted earlier, the moment is the quantity which can be determined accurately by observations, whereas the stress drop is typically inferred from formulae like (7) which assume that the fault is a single isolated zone. Thus it is perhaps more relevant for observations to determine for a fixed moment and fault length

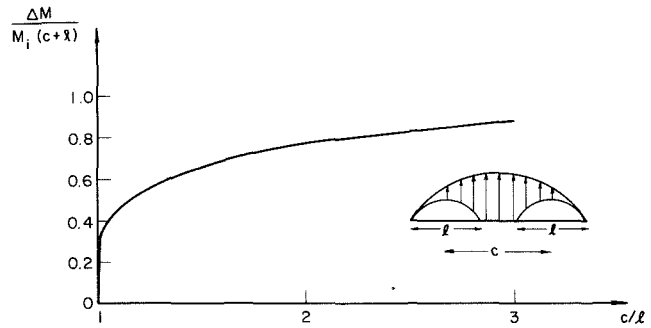

Fig. 8. Moment due to failure of asperity between two slip zones divided by the moment due to uniform stress drop on an isolated slip zone of length $c + l$.

the ratio between the actual stress drop and the apparent stress drop inferred from (7). Equating the moments calculated from (6) by using (15) with $\tau = \Delta\tau_{true}$ and from (7) with $l = 2b$ and $\tau = \Delta\tau_{app}$ yields

$$\frac{\Delta\tau_{true}}{\Delta\tau_{app}} = \frac{1}{1 + (a/b)^2 - 2\lambda^2} \tag{17}$$

The reciprocal of this expression is plotted versus c/l [$=(1 + a/b)/(1 - a/b)$] in Figure 7. For very small asperity lengths the two stress drops are approximately equal, but more generally the apparent stress drop can significantly underestimate the true stress drop. For example, if $c/l = 1.2$, the true stress drop is roughly twice the apparent value, but if the asperity length is equal to the length of the adjacent slip zones ($c/l = 2$), the apparent stress drop is only 24% of the true stress drop.

Rice [1979*b*] has used results for the infinite periodic array of collinear cracks to obtain a formula corresponding to (17) for a large number of segments. Rice's expression is (in our notation)

$$\frac{\Delta\tau_{true}}{\Delta\tau_{app}} = \frac{n\pi^2}{8 \ln\left[\sec\frac{\pi}{2}(1 - l/c)\right]} \tag{18}$$

where $n \gg 1$ is the number of slip zone segments. For $c/l = 1.01$, 1.1, 1.2, and 1.5 this ratio is $0.30n$, $0.63n$, $0.91n$, and $1.78n$, respectively. (The numerical values given by *Rice* [1979*b*] for $(1 - l/c) = 0.25$, 0.1, and 0.01 are in error and should be replaced by $1.28n$, $0.67n$, and $0.30n$, respectively.) Comparison of (18) with (17) reveals that the difference between the actual and apparent stress drops is greater for the larger numbers of slip zone segments. For $c/l = 1.2$, $\Delta\tau_{true} = 2\,\Delta\tau_{app}$ for two segments, but for a large number of segments, say, 20–25, the actual stress drop in each segment is 20–25 times the apparent value.

The calculations in this section give specific numerical examples of the general result obtained by *Madariaga* [1979]: for a given moment and fault length the segmented fault represented by the barrier model has high stress drop than the isolated fault.

Asperity Model

In this section we demonstrate that the failure of an asperity, which may occupy a very small portion of the fault plane, can cause a relatively large moment because of the additional displacement induced on the adjacent slip zones. Because the body has been assumed to be linearly elastic, this moment is simply equal to the difference

$$\Delta M = M_i(c + l) - M_2 \tag{19}$$

where M_2 is given by (16) and $M_i(l)$ is given by (7). This difference divided by $2M_i(l)$ is the difference between the two curves in Figure 6, and in Figure 8, $\Delta M/M_i(c + l)$ is plotted as a function of c/l. (For fixed stress drop, $M_2/M_i(c + l)$ is equal to the reciprocal of the right-hand side of (17) so that Figure 7 is also a plot of $1 - \Delta M/M_i(c + l)$.)

For values of c/l greater than about 2, the ratio $\Delta M/M_i(c + l)$ is roughly unity, and the moment ΔM differs from $M_i(c + l)$ by less than 20%. Thus if the asperity length is greater than about one third of the total length which slips during failure of the asperity, the effect of the preexisting slip zones on the moment is relatively small (Figure 8). Note, however, that the moment due to failure of the asperity can be relatively large even if the asperity is very small. For example, when the asperity length is only 5% of the preexisting slip zone length (for $c/l = 1.05$, the asperity length is 2% of the total length which slips during failure of the asperity), the moment due to failure of the asperity is 1.8 times the moment due to creating an isolated slip zone of length l or about 40% of the moment due to breaking the entire slip zone of length $c + l$. As mentioned earlier, this relatively large moment is due to the additional displacement induced on the already existing slip zones. Because the strength of these zones has already been reduced to the residual friction level τ_f, these portions of the fault plane undergo zero stress drop during the failure of the asperity. The effect of this on the average stress drop will be examined next.

If the slip zones are widely separated, the stress on the asperity will be roughly equal to the value of the stress applied in the far field (τ_∞) except very near the edges of the slip zones. Consequently, failure of the asperity will be accompanied by a stress drop approximately equal to $\tau_\infty - \tau_f$. If, however, the slip zones are closer together, the average stress on the asperity will exceed τ_∞ (as demonstrated by Figure 5), and the corresponding stress drop due to failure of the asperity is increased. Of course, the case of most interest is when the asperity between the slip zones is small by comparison to the slip zone length because this is the case for which the presence of the neighboring slip zones is likely to induce failure of the asperity. Specifically, the calculations will demonstrate that the stress drop averaged over the area of a small asperity can be very large, whereas the average over the entire zone which slips (during failure of the asperity) is small.

For the two collinear slip zones shown in Figure 4*a*, the stress on the plane between the slip zones can be determined from expressions given by *Erdogan* [1962]. The result is

$$\tau_{asp} = (\tau_\infty - \tau_f)\frac{(b^2\lambda^2 - x^2)}{[(a^2 - x^2)(b^2 - x^2)]^{1/2}} + \tau_f \tag{20}$$

where $-a < x < a$, τ_∞ is the stress applied in the far field, τ_f is the residual friction stress, and $\lambda^2 = E(m)/F(m)$. Because the stress in the asperity is assumed to be reduced to τ_f by failure, the stress drop is simply given by the first term of (20). Consequently, the average stress drop in the asperity is simply

$$\Delta\bar{\tau}_{asp} = \frac{\tau}{a}\int_0^a \frac{(b^2\lambda^2 - x^2)\,dx}{[(a^2 - x^2)(b^2 - x^2)]^{1/2}} \tag{21}$$

where $\tau = \tau_\infty - \tau_f$. This integral can be expressed as [*Abramowitz and Stegun,* 1964, p. 596, equation 17.3.13]

$$\Delta\bar{\tau}_{asp} = \tau(b/a)[(2/\pi)F(m)]^{-1} \tag{22}$$

Because the stress on other portions of the slip zones has already been reduced to τ_f, the stress drop here is zero (although there is, of course, additional slip caused by failure of the asperity). Consequently, the average stress drop for the entire slip zone is obtained by multiplying (22) by a/b or

$$\Delta\bar{\tau}_{flt} = \tau[(2/\pi)F(m)]^{-1} \tag{23}$$

This relation between the average stress drop in the asperity and the average stress drop of the slip zone is a special case of the more general relation established by Madariaga. (See equation (15) of *Madariaga* [1979].) It is straightforward to demonstrate from the properties of $F(m)$ [e.g., *Abramowitz and Stegun,* 1964, equation 17.3.26] that $\Delta\bar{\tau}_{asp}$ approaches infinity as a/b approaches zero (or $c/l = 1$), but that $\Delta\bar{\tau}_{flt} = 0$ in this same limit. Thus although the local stress drop in the asperity can be large, it occurs over such a small area that its contribution to the average stress drop of the entire fault is very small. $\Delta\bar{\tau}_{flt}/\tau$ and $(\Delta\bar{\tau}_{asp}/\tau)^{-1}$ are plotted in Figure 9.

The stress drop defined by (20) is the true stress drop, that is, the stress on the fault plane prior to slip minus that after slip. As noted earlier, the true stress drop is generally not known; rather an apparent stress drop is inferred from (7). Thus, letting $\tau = \Delta\tau_{app}$ and $l = 2b$ in the right-hand side of (7) and setting the left-hand side equal to ΔM yield

$$\Delta\tau_{app} = \tau[2\lambda^2 - (a/b)^2] \tag{24}$$

The ratio of the apparent stress drop to the true average stress drop is

$$\frac{\Delta\tau_{app}}{\Delta\bar{\tau}_{flt}} = \frac{2}{\pi}[2E(m) - (1 - m^2)F(m)] \tag{25}$$

where $m^2 = 1 - a^2/b^2$. This ratio varies monotonically from unity when $c/l = 1$ (i.e., $a/b = 0$) to $4/\pi$ when $c/l = \infty$ ($a/b = 1$). Hence the apparent stress drop calculated from (7) is a good estimate for the true average stress drop.

Although the apparent stress drop does not differ greatly from the true average stress drop, both quantities underestimate the effective stress for small values of c/l. For $c/l = 1.01$, $\Delta\tau_{app}$ underestimates the effective stress by a factor of more than 3 and $\Delta\bar{\tau}_{flt}$ by a factor of more than 5. Hence if the stress drop is assumed equal to the effective stress (as is the case for an isolated zone) for the purpose of computing W_0 from (10), this quantity may be underestimated by a significant amount. If, however, $c/l > 1.2$, $\Delta\tau_{app}$ agrees with the effective stress to a factor of 2, and the difference is probably not significant.

Concluding Discussion

Although our model is too simple to describe a real fault in detail, it does make it possible to evaluate quantitatively the effects of the interaction of slip zones separated by asperities. The results are not surprising, but they do demonstrate the dramatic effects that small strong asperities can have on fault processes. In particular, the failure of a small strong asperity can cause a relatively large moment. This result is primarily due to the additional displacement, which is induced by failure of the asperity, on the adjacent already weakened slip zones. Consequently, slip on these zones might be said to 'prepare' the fault for large relative displacements due to failure of the strong asperity. The failure of such an asperity can be associated with a large local stress drop, but the stress drop when averaged over the entire slipping region is approximately equal to the stress drop obtained by assuming slip occurred on an isolated fault of the same moment and length. This result suggests itself as a possible explanation for why the observed stress drops for large earthquakes (which are usually an average over the entire slipping region) are relatively constant despite possible heterogeneity of the fault zone [e.g., *Kanamori and Anderson,* 1975]. Moreover, unless the ratio of asperity size to fault length is very small, this stress drop is a good estimate (within a factor of 2) of the effective stress ($\tau_\infty - \tau_f$) and hence yields a good estimate of the strain energy change when used in the usual formula for an isolated fault.

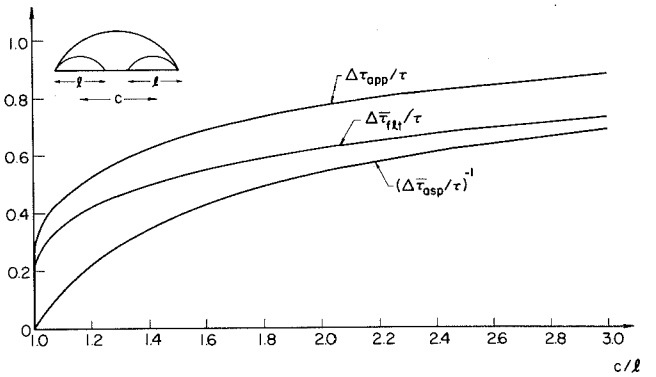

Fig. 9. Average stress drop due to failure of the asperity between two collinear slip zones divided by effective stress as a function of c/l. $\Delta\bar{\tau}_{asp}$ is the stress drop averaged over the width of the asperity (note that the reciprocal of $\delta\bar{\tau}_{asp}/\tau$ is plotted) and $\Delta\bar{\tau}_{flt}$ is the stress drop averaged over the entire region which slips (see (22) and (23)). $\Delta\bar{\tau}_{app}$ is the apparent stress drop inferred by assuming uniform stress drop on an isolated fault of length $c + l$.

For convenience of analysis the fault plane has been idealized as consisting of regions which slip freely at a uniform residual value of the friction stress and of regions which slip only at the time of an earthquake. In actuality, there is likely to be a distribution of strength on the fault plane and a relatively continuous variation of the slipping regions as the tectonic stress is increased. Of course, the interactions in this case will be much more complicated than those described here. Nevertheless, the idealization considered here is a limiting one and hence can reasonably be considered to yield bounds for intermediate situations. Moreover, there is evidence from direct observation of fault surfaces associated with seismic events in mines [*McGarr et al.,* 1979*a*] that fault slip zones, at least in some instances, may not be planar. Again the analysis of this case is more complicated than that presented here, but some preliminary results have been obtained by *Segall and Pollard* [1980] and by *McGarr et al.* [1979*b*]. Three-dimensional effects may also be important, and Madariaga has given some general results which are applicable in this case. Although for the three-dimensional case there appears to be no simple calculation analogous to that presented here, *McGarr* [1981] has recently considered an approximate solution for an annular fault model. His predictions are comparable to those given here if the results are compared on the basis of fault area. More generally, the development of a fault plane may be a late stage in a process of inelastic deformation in a large re-

gion. In this case an inclusion model like that suggested by *Rudnicki* [1977] may be appropriate, and the development of a fault may occur by the localization processes which were analyzed by *Rudnicki and Rice* [1975]. Indeed, *Rice* [1978] has suggested that the observations of *Lindh et al.* [1978] on the orientation of foreshocks relative to mainshock are consistent with this latter analysis. However, this misorientation may be related to the principal stress axes rotation caused by the foreshocks themselves [*Rudnicki,* 1979].

This analysis has also assumed that failure results in a reduction of the stress to the residual friction value. In general, the stress may not be reduced to this value upon failure, and consequently the friction stress on the fault plane will not be uniform. A limiting case is the model of *Das and Aki* [1977*a*, *b*] in which a propagating fault can leave unbroken ligaments behind its tip. The calculations given here for the barrier model are relevant to this case, but they are purely kinematic in nature, and for a more detailed analysis it would be necessary to introduce a fracture criteria. Moreover, for fault lengths which are comparable to the distance to the free surface or boundary of the seismogenic region, the details of propagation are likely to be affected by whether the boundary conditions are idealized as prescribed displacements or stresses [*Freund,* 1979].

In spite of all the limitations of the present analysis, it is useful in demonstrating the magnitude of the effects that interacting slip zones may have in fault processes.

APPENDIX

The relative displacement for the two collinear slip zones (Figure 4*b*) can be shown from expressions given by *Erdogan* [1962] to be

$$\delta(x) = 2(1-\nu)\tau\mu^{-1}\int_x^b \frac{(s^2-b^2\lambda^2)\,ds}{[(s^2-a^2)(b^2-s^2)]^{1/2}}$$

where $\lambda^2 = E(m)/F(m)$, $m^2 = 1 - a^2/b^2$, and $E(m)$ and $F(m)$ are the complete elliptic integrals defined following (11). This integral can be expressed as

$$\delta(x) = 2(1-\nu)\tau\mu^{-1}b[E(\phi, m) - \lambda^2 F(\phi, m)] \qquad \text{(A1)}$$

where

$$F(\phi, m) = \int_0^\phi (1 - m^2\sin^2\phi)^{-1/2}\,d\theta$$

$$E(\phi, m) = \int_0^\phi (1 - m^2\sin^2\theta)^{1/2}\,d\theta$$

are elliptic integrals of the first and second kinds, respectively [*Abramowitz and Stegun,* 1964], and

$$\sin^2\phi = m^{-2}[1 - (x/b)^2]$$

The average displacement is simply the integral of $\delta(x)$ divided by $b - a$. Evaluation of the integral can be accomplished by using the results of *Tranter* [1961] or of *Lowengrub and Srisvastava* [1968] for the corresponding tensile crack problem, and the final expression can be written in the form of (15).

Acknowledgments. Helpful discussions of one of us (J.W.R.) with J. R. Rice are gratefully acknowledged. This work was supported by U.S. Geological Survey contract 14-08-0001-19146 at the University of Illinois, by the Earth Sciences Section, National Science Foundation grants EAR78-11973 and EAR77-13641, and U.S. Geological Survey contract 14-08-0001-18371 at the Seismological Laboratory of the California Institute of Technology, and by the U.S. Geological Survey while J. W. Rudnicki was geophysicist at the U.S. Geological Survey Center for Earthquake Studies, Menlo Park, California, during June 1979. Division of Geological and Planetary Sciences, California Institute of Technology contribution 3425.

REFERENCES

Abramowitz, M., and I. A. Stegun (Eds), *Handbook of Mathematical Functions, Appl. Math. Ser. 55,* National Bureau of Standards, Washington, D. C., 1964.

Aki, K., Characterization of barriers on an earthquake fault, *J. Geophys. Res., 84,* 6140–6148, 1979.

Barenblatt, G. I., Mathematical theory of equilibrium cracks in brittle fracture, *Adv. Appl Mech., 7,* 55–129, 1962.

Barton, N., A model study of rock joint deformation, *Intl. J. Rock Mech. Min. Sci., 9,* 579–602, 1972.

Barton, N., Review of a new strength criterion for rock joints, *Eng. Geol., 7,* 287–332, 1973.

Bowden, F. P., and D. Tabor, *Friction: An Introduction to Tribology,* 178 pp., Anchor Books, Garden City, N. Y., 1973.

Das, S., and K. Aki, A numerical study of two dimensional spontaneous rupture propagation, *Geophys. J. R. Astron. Soc., 50,* 643–668, 1977*a*.

Das, S., and K. Aki, Fault plane with barriers: A versatile earthquake model, *J. Geophys. Res., 82,* 5658–5670, 1977*b*.

Erdogan, F., On stress distribution in plates with collinear cuts under arbitrary loads, in *Proceedings of the 4th U.S. National Congress on Applied Mechanics,* Vol. 1, edited by R. M. Rosenberg, pp. 547–553, American Society of Mechanical Engineers, Berkeley, Calif., 1962.

Freund, L. B., The mechanics of dynamic shear crack propagation, *J. Geophys. Res., 84,* 2199–2209, 1979.

Imamura, A., *Theoretical and Applied Seismology,* 348 pp., Maruzen, Tokyo, 1937.

Irwin, G. R., Analysis of stresses and strains near the end of a crack transversing a plate, *J. Appl. Mech., 24,* 361–364, 1957.

Ishida, M., and H. Kanamori, The foreshock activity of the 1971 San Fernando, California earthquake, *Bull. Seismol. Soc. Am., 68,* 1265–1279, 1978.

Ishida, M., and H. Kanamori, Temporal variation of seismicity and spectrum of small earthquakes preceding the 1952 Kern County, California earthquake, *Bull. Seismol. Soc. Am., 70,* 509–528, 1980.

Jaeger, J. C., and N. G. W. Cook, *Fundamentals of Rock Mechanics,* 2nd ed., 585 pp., Halsted, New York, 1976.

Jones, L. M., and P. Molnar, Some characteristics of foreshocks and their possible relationship to earthquake prediction and premonitory slip on faults, *J. Geophys. Res., 84,* 3496–3608, 1979.

Kanamori, H., The energy release in great earthquakes, *J. Geophys. Res., 82,* 2981–2987, 1977.

Kanamori, H., Use of seismic radiation to infer source parameters, Proceedings of Conference III, Fault Mechanics and Its Relation to Earthquake Prediction, *Geol. Surv. Open File Rep. U.S., 78-380,* 283–318, 1978.

Kanamori, H., and D. L. Anderson, Theoretical basis of some empirical relations in seismology, *Bull. Seismol. Soc. Am., 65,* 1073–1095, 1975.

Kanamori, H., and G. S. Stewart, Seismological aspects of the Guatemala earthquake of February 4, 1976, *J. Geophys. Res., 83,* 3427–3434, 1978.

Knott, J. F., *Fundamentals of Fracture Mechanics,* 273 pp., Halsted, New York, 1973.

Koiter, W. T., An infinite row of collinear cracks in an infinite elastic sheet, *Ing. Arch., 28,* 168–172, 1959.

Kostrov, B. V., Seismic moment, energy of earthquakes, and seismic flow of rock, *Izv. Acad. Sci. USSR Phys. Solid Earth, 1,* 23–40, 1974.

Lay, T., and H. Kanamori, Earthquake doublets in the Solomon Islands, *Phys. Earth Planet. Inter., 21,* 283–304, 1980.

Lindh, A., G. Fuis, and C. Mantis, Seismic amplitude measurements suggest foreshocks have different focal mechanisms than aftershocks, *Science, 201,* 56–58, 1978.

Love, A. E. H., *A Treatise on the Mathematical Theory of Elasticity,* Dover, New York, 643 pp., 1927. (Reprint of 4th ed., Cambridge University Press, New York, 1944.)

Lowengrub, M., and K. N. Srivastava, On two planar Griffith cracks in an infinite elastic solid, *Intl. J. Eng. Sci., 6,* 349–362, 1968.

Madariaga, R., Implications of stress-drop models of earthquakes for the inversion of stress drop from seismic observations, *Pure Appl. Geophys., 115,* 301–316, 1977.

Madariaga, R., On the relation between seismic moment and stress drop in the presence of stress and strength heterogeneity, *J. Geophys. Res., 84,* 2243–2250, 1979.

McGarr, A., Analysis of peak ground motion in terms of a model of inhomogeneous faulting, *J. Geophys. Res.,* in press, 1981.

McGarr, A., S. M. Spottiswoode, N. C. Gay, and W. D. Ortlepp, Observations relevant to seismic driving stress, stress drop, and efficiency, *J. Geophys. Res., 84,* 2251–2263, 1979*a*.

McGarr, A., D. Pollard, N. C. Gay, and W. D. Ortlepp, Observations and analysis of structures in exhumed mine-induced faults, Proceedings of Conference VIII, Analysis of Actual Fault Zones in Bedrock, *Geol. Surv. Open File Rep. U.S., 79-1239,* 101–120, 1979*b*.

Mikumo, T., and T. Miyatake, Earthquake sequences on a frictional fault model with non-uniform strengths and relaxation times, *Geophys. J. R. Astron. Soc., 59,* 497–522, 1979.

Miyamura, S., S. Omote, R. Teisseyre, and E. Vesanen, Multiple shocks and earthquakes series pattern, *Bull. Intl. Inst. Seismol. Earthquake Eng., 2,* 71–92, 1964.

Muskhelishvili, N. I., *Some Basic Problems of the Mathematical Theory of Elasticity,* translated from Russian by J. R. M. Radok, Noordhoff, Groningen, Netherlands, 1953.

Nagamune, T., Source regions of great earthquakes, *Geophys. Mag., 35,* 333–399, 1971.

Orowan, E., Mechanism of seismic faulting, *Mem. Geol. Soc. Am., 79,* 323–345, 1960.

Rial, J. A., The Caracus, Venezuela, earthquake of July, 1962: multiple-source event, *J. Geophys. Res., 83,* 5405–5414, 1978.

Rice, J. R., An examination of the fracture mechanics energy balance from the point-of-view of continuum mechanics, in *Proceedings of the 1st International Conference on Fracture,* vol. 1, edited by T. Yokobori, pp. 283–308, Japanese Society for Strength and Fracture, Sendai, Japan, 1966.

Rice, J. R., Mathematical analysis in the mechanics of fracture, in *Fracture: An Advanced Treatise,* vol. 2, eidted by H. Liebowitz, pp. 191–311, Academic, New York, 1968.

Rice, J. R., Models for the inception of earthquake rupture, *Eos Trans. AGU, 59,* 1204, 1978.

Rice, J. R., Theory of precursory processes in the inception of earthquake rupture, *Gerlands Beitr. Geophys., 88,* 91–127, 1979*a*.

Rice, J. R., The mechanics of earthquake rupture, in *Proceedings of the International School of Physics, 'Enrico Fermi,' Italian Physical Society, Course LXX VIII on Physics of the Earth's Interior,* edited by E. Boschi, North Holland, Amsterdam, in press, 1979*b*.

Richter, C. F., *Elementary Seismology,* 768 pp., W. F. Freeman, San Francisco, Calif., 1958.

Rudnicki, J. W., The inception of faulting in a rock mass with a weakened zone, *J. Geophys. Res., 82,* 844–854, 1977.

Rudnicki, J. W., The stabilization of slip on a narrow weakening fault zone by coupled deformation-pore fluid diffusion, *Bull. Seismol. Soc. Am., 69,* 1011–1026, 1979*a*.

Rudnicki, J. W., Rotation of principal stress axes caused by faulting, *Geophys. Res. Lett., 6,* 135–138, 1979*b*.

Rudnicki, J. W., Fracture mechanics applied to the earth's crust, *Annu. Rev. Earth Planet Sci., 8,* 489–525, 1980.

Rudnicki, J. W., and J. R. Rice, Conditions for the localization of deformation in pressure-sensitive dilatant materials, *J. Mech. Phys. Solids, 23,* 371–394, 1975.

Segall, P., and D. D. Pollard, Mechanics of discontinuous faults, *J. Geophys. Res., 85,* 4337, 1980.

Tada, H., P. C. Paris, G. R. Irwin, *The Stress Analysis of Cracks Handbook,* Del Research Corporation, Hellertown, Pa., 1973.

Tranter, C. J., The opening of a pair of coplanar Griffith cracks under internal pressure, *Q. J. Mech. Appl. Math., 14,* 283–292, 1961.

Trifunac, M. D., and J. N. Brune, Complexity of energy release during Imperial Valley, California earthquake of 1940, *Bull. Seismol. Soc. Am., 60,* 137–160, 1970.

Willmore, T. J., The distribution of stress in the neighborhood of a crack, *Q. J. Mech. Appl. Math., 2,* 53–63, 1949.

Wyss, M., and J. N. Brune, The Alaska earthquake of 28 March, 1964: A complex multiple rupture, *Bull. Seismol. Soc. Am., 57,* 1017–1023, 1967.

(Received March 7, 1980;
revised September 2, 1980;
accepted September 22, 1980.)